Inorg. Chem. **2008**, *47*, 4023−4031

Binuclear Copper(II) Complexes with N_4O_3 Coordinating Heptadentate Ligand: Synthesis, Structure, Magnetic Properties, Density-Functional Theory Study, and Catecholase Activity

Atanu Banerjee,[†] Sumana Sarkar,[†] Deepak Chopra,[‡] Enrique Colacio,[§] and Kajal Krishna Rajak[†,*]

Inorganic Chemistry Section, Department of Chemistry, Jadavpur University, Kolkata 700 032, India, Solid State and Structural Chemistry Unit, Indian Institute of Science, Bangalore 560 012, India, and Departamento de Química Inorgánica, Facultad de Ciencias, Universidad de Granada, 18071 Granada, Spain

Received August 10, 2007

The N_4O_3 coordinating heptadentate ligand afforded binuclear complex $[Cu_2(H_2L)(\mu\text{-OH})](ClO_4)_2$ (**1**) and $[Cu_2(L)(H_2O)_2]PF_6$ (**2**). In complex **1**, two copper ions are held together by μ-phenoxo and μ-hydroxo bridges, whereas in complex **2**, the copper centers are connected only by a μ-phenoxo bridge. In **1**, both the Cu(II) centers have square pyramidal geometry ($\tau = 0.01-0.205$), whereas in the case of **2**, one Cu(II) center has square pyramidal ($\tau = 0.2517$) and other one has square based pyramidal distorted trigonal bipyramidal ($\tau = 0.54$) geometry. Complexes **1** and **2** show an strong intramolecular and very weak antiferromagnetic interaction, respectively. Density-functional theory calculations were performed to establish the magneto structural correlation between the two paramagnetic copper(II) centers. Both of the complexes display a couple of one-electron reductive responses near −0.80 and −1.10 V. The complexes show significant catalytic activity at pH 8.5 on the oxidation of 3,5-di-*tert*-butylcatechol (3,5-DTBC) to 3,5-di-*tert*-butylquinone (3,5-DTBQ), and the activity measured in terms of $k_{cat} = 29-37\ h^{-1}$.

Introduction

Binuclear copper (II) complexes have an important functional role in many metalloenzymes,[1] a noteworthy example being catechol oxidase.[2] It catalyzes the oxidation of *o*-diphenol to the corresponding *o*-quinone coupled with $2e/2H^+$ reduction of O_2 to H_2O.[3] The X-ray structure of catechol oxidase isolated from sweet potato[4] reveals that it contains antiferromagnetically coupled electron paramagnetic resonance (EPR) silent binuclear copper(II) centers in which the Cu···Cu distance is 2.9 Å. In the coordination sphere of isolated catechol oxidase, each copper(II) is coordinated to three histidine nitrogen atoms followed by an exogenous bridging hydroxide group forming a four coordinated trigonal pyramidal geometry. Thus, the copper(II) species using binuclear complex forming ligands have attracted increasing attention in recent years.[5–7] Besides the chemistry of biologically relevant polynuclear complexes of copper, the study of variable temperature magnetic moment is also important to examine the type of magnetic interaction involved in such species. The theoretical interpretation of magnetic behavior by the density-functional theory (DFT) method[8] is an emerging field of research of the pathways of magnetic exchange

* To whom correspondence should be addressed. E-mail: kajalrajak@hotmail.com.
† Jadavpur University.
‡ Indian Institute of Science.
§ Universidad de Granada.

(1) Linder, M. C.; Goode, C. A. *Biochemistry of Copper*; Plenum: New York, 1991.
(2) Tremolieres, M.; Bieth, J. B. *Phytochemistry* **1984**, *23*, 501.
(3) (a) Sanchez-Ferrer, A.; Rodriguez-Lopez, J. N.; Garcia-Canovas, F.; Garcia-Carmona, F. *Biochim. Biophys. Acta* **1995**, *1247*, 1. (b) Solomon, E. I.; Sundaram, U. M.; Machonkin, T. E. *Chem. Rev.* **1996**, *96*, 2563. (c) Reim, J.; Krebs, B. *J. Chem. Soc., Dalton Trans.* **1997**, 3793. (d) Eicken, C.; Krebs, B.; Sacchettini, J. C. *Curr. Opin. Struct. Biol.* **1999**, *9*, 677. (e) Gerdemann, C.; Eicken, C.; Krebs, B. *Acc. Chem. Res.* **2002**, *35*, 183. (f) Torelli, S.; Belle, C.; Hamman, S.; Pierre, J.-L.; Saint-Aman, E. *Inorg. Chem.* **2002**, *41*, 3983.
(4) Klabunde, T.; Eicken, C.; Sacchettini, J. C.; Krebs, B. *Nat. Struct. Biol.* **1998**, *5*, 1084.
(5) (a) Latour, J. M. *Bull. Soc. Chim. Fr.* **1988**, 508. (b) Sorrell, T. N. *Tetrahedron* **1989**, *45*, 3. (c) Vigato, P. A.; Tamburini, S.; Fenton, D. *Coord. Chem. Rev.* **1990**, *106*, 25. (d) Kitajima, N. *Adv. Inorg. Chem.* **1992**, *39*, 1. (e) Karlin, K. D.; Tyekler, Z. *Bioinorganic Chemistry of Copper*; Chapman and Hill: New York, 1993. (f) Holz, R. C.; Brink, J. M.; Gobena, F. T.; O'Connor, C. J. *Inorg. Chem.* **1994**, *33*, 6086. (g) Holz, R. C.; Bradshaw, J. M.; Bennet, B. *Inorg. Chem.* **1998**, *37*, 1219.

10.1021/ic7015935 CCC: $40.75 © 2008 American Chemical Society
Published on Web 04/16/2008

interactions as well as the electronic structure of the biologically relevant coordination compounds. The above state of development has generated a lot of interest in the search of new binuclear copper(II) complexes using a N_4O_3 coordinating heptadentate ligand.

In this article we will describe the synthesis, characterization, magnetic properties, and DFT calculation of two binuclear copper(II) complexes. The oxidation of catechol to quinone is scrutinized.

Experimental Section

Materials. All the starting chemicals were analytically pure and used without further purification. The ligands were prepared according to the literature procedure.[9]

Caution! *Perchlorate salts are highly explosive, and should be handled with care and in small amounts.*

Physical Measurements. UV−vis spectra were recorded on a Perkin-Elmer LAMBDA 25 spectrophotometer, and IR spectra were measured with a Perkin-Elmer L-0100 spectrometer. Electrochemical measurements were performed (acetonitrile solution) on a CH 620A electrochemical analyzer using a platinum electrode. Tetraethylammonium perchlorate (TEAP)[10] was used as a supporting electrolyte, and the potentials are referenced to the saturated calomel electrode (SCE) without junction correction. The cyclic voltammograms were recorded with a scan rate of 50 mV/s with *iR* compensation in all cases. EPR experiments were performed on a Varian E-109C (X band, 9.1 GHz) spectrometer at a microwave power of 30 dB and modulation amplitude of 12.5 gauss, and spectra were collected using a quartz dewar flask. Diphenylpicrylhydrazyl (dpph, $g = 2.0037$) was used to calibrate the spectra. Magnetic measurements were carried out on polycrystalline samples with a Quantum Design MPMS XL SQUID susceptometer operating at a magnetic field of 0.1 T between 2 and 300 K. The diamagnetic corrections were evaluated from Pascal's constants. Elemental analyses (C, H, N) were performed on a Perkin-Elmer 2400 Series II elemental analyzer.

DFT Study and Computational Details. DFT study has proven to be an important tool to obtain better insights into the electronic structure energy and the magnetic exchange mechanism in various transition metal based magnetic systems. Thus, DFT calculations using the X-ray coordinates of the cationic part of the complex **1** has been done to understand the exchange pathway. The exchange coupling constant of the cationic part of **2** was calculated using both the X-ray coordinates and the optimized geometry because the experimental *J* value is very small. The optimization of the cationic part of **2** was done using the basis sets 6−31 g (H), 6−31+g (C, N, and O), and 6−311+g(d) (Cu). The magnetic exchange interaction between the transition metal ions is studied on the basis of DFT coupled with the broken symmetry approach[11] for weakly interacting magnetic ions. The exchange coupling constant *J* for a two center magnetic ion can be evaluated according to the following equation:

$$E_{HS} - E_{BS} = -(2S_1S_2 + S_2)J \quad (1)$$

where S_1 and S_2 stand for the total spin for the paramagnetic centers; in the case of $S_1 = S_2 = 1/2$, $E_{HS} - E_{BS} = -J$, using the Heisenberg Hamiltonian, $\hat{H} = -J\hat{S}_1\hat{S}_2$.

The term E_{HS} corresponds to the energy of the triplet state, and the term E_{BS} to the broken-symmetry (BS) state. The positive and the negative value of the coupling constant *J* indicates the ferromagnetic and antiferromagnetic ground states of the system, respectively.

It has been cited in the literature that exchange coupling constants *J* are often overestimated in DFT calculation.[12] In a few cases[12a,e] the calculated *J* for weakly coupled systems using BS gives exchange coupling constants differing both in sign and values from the experimentally observed values. Despite of that, in BS calculations the molecule is treated as two weakly coupled monomers, and hence, the BS solution is very useful to understand the exchange pathways for polynuclear transition metal complexes.[13] Thus, in present case we have performed the DFT calculation with the BS solution for monitoring the exchange pathways involved in the system.

Ground state electronic structure calculations of the complexes have been carried out using DFT[14] methods with the Gaussian 03 program.[15] Becke's hybrid function[16] with the Lee−Yang−Parr (LYP) correlation function[17] was used through the study. We employed a triple-ζ quality all-electron basis set for copper atoms (TZP),[18] a double-ζ all-electron basis set[19] for C, N, and O, and a 6−31G basis set for H. In other calculations instead of a triple-ζ quality all-electron basis set for copper atoms, LANL2DZ valence and effective core potential functions were used. All energy calculations were performed using the self-consistent field "tight" option of the Gaussian 03 program to ensure sufficiently well converged values for the state energies.

(6) (a) Neves, A.; Rossi, L. M.; Vencato, I.; Drago, V.; Hasse, W.; Werner, R. *Inorg. Chim. Acta* **1998**, *281*, 111. (b) Torelli, S.; Belle, C.; Gautier-Luneau, I.; Pierre, J. L.; Saint-Aman, E.; Latour, J. M.; LePape, L.; Luneau, D. *Inorg. Chem.* **2000**, *39*, 3526. (c) Neves, A.; Rossi, L. M.; Bortoluzzi, A. J.; Mangrich, A. S.; Hasse, W.; Werner, R. *J. Braz. Chem. Soc.* **2001**, *12*, 747. (d) Dapporto, P.; Formica, M.; Fusi, V.; Giorgi, L.; Micheloni, M.; Paoli, P.; Pontellini, R.; Rossi, P. *Inorg. Chem.* **2001**, *40*, 6186. (e) Fondo, F.; Gartia-Deibe, A. M.; Sanmartin, J.; Bermejo, M. R.; Lezama, L.; Rojo, T. *Eur. J. Inorg. Chem.* **2003**, 3703.

(7) (a) Peralta, R. A.; Neves, A.; Bortoluzzi, A. J.; Anjos, A. dos.; Xavier, F. R.; Szpoganicz, B.; Terenzi, H.; de Oliveira, M. C. B.; Castellano, E.; Friedermann, G. R. d.; Mangrich, A. S.; Novak, M. A. *J. Inorg. Biochem.* **2006**, *100*, 992. (b) Weng, C. H.; Cheng, S. C.; Wei, H. M.; Wei, H. H.; Lee, C. J. *Inorg. Chim. Acta* **2006**, *359*, 2029. (c) Rey, N. A.; Neves, A.; Bortoluzzi, A. J.; Pich, C. T.; Terenz, H. *Inorg. Chem.* **2007**, *46*, 348. (d) Ackermann, J.; Buchler, S.; Meyer, F. *C. R. Chim.* **2007**, *10*, 421.

(8) (a) Kahn, O. *Molecular Magnetism*; VCH Publishers: New York, 1993. (b) Rodriguez, J. H.; Mc Cusker, J. K. *J. Chem. Phys.* **2002**, *116*, 6253. (c) Ruiz, E.; Alvarez, S. *ChemPhysChem* **2005**, *6*, 1094. (d) Ruiz, E.; Rodriguez-Fortea, A.; Tercero, J.; Cauchy, T. *J. Chem. Phys.* **2005**, *123*, 74102.

(9) Mondal, A.; Sarkar, S.; Chopra, D.; Guru Row, T. N.; Pramanik, K.; Rajak, K. K. *Inorg. Chem.* **2005**, *44*, 703.

(10) Lahiri, G. K.; Bhattacharya, S.; Ghosh, B. K.; Chakravorty, A. *Inorg. Chem.* **1987**, *26*, 4324.

(11) (a) Noodleman, L. *J. Chem. Phys.* **1981**, *74*, 5737. (b) Noodleman, L.; Baerends, E. J. *J. Am. Chem. Soc.* **1984**, *106*, 2316. (c) Noodleman, L.; Case, D. A. *Adv. Inorg. Chem.* **1992**, *38*, 423.

(12) (a) Zhao, X. G.; Richardson, W. H.; Chen, J. L.; Noodleman, L.; Tasi, H. L.; Hendrickson, D. N. *Inorg. Chem.* **1997**, *36*, 1198. (b) Bencini, A.; Totti, F.; Daul, C. A.; Doclo, K.; Fantucci, P.; Barone, V. *Inorg. Chem.* **1997**, *36*, 5022. (c) Adamo, C.; Barone, V.; Bencini, A.; Totti, F.; Ciofini, I. *Inorg. Chem.* **1999**, *38*, 1996. (d) Soda, T.; Kitagawa, Y.; Onishi, T.; Yakano, Y.; Shigeta, Y.; Nagao, H.; Yoshioka, Y.; Yamaguchi, K. *Chem. Phys. Lett.* **2000**, *319*, 223. (e) Prushan, M. J.; Tomezsko, D. M.; Lofland, S.; Zeller, M.; Hunter, A. D. *Inorg. Chim. Acta* **2007**, *360*, 2245.

(13) (a) Noodleman, L.; Morman, J. G. *J. Chem. Phys.* **1979**, *70*, 4903. (b) Mc Grady, J. E.; Stranger, R. *J. Am. Chem. Soc.* **1997**, *119*, 8512.

(14) Parr, R. G.; Yang, W. *Density Functional Theory of Atoms and Molecules*; Oxford University Press: Oxford, 1989.

Crystallographic Studies. Single crystals of suitable quality for single crystal X-ray diffraction studies on the complex $[Cu_2(H_2L)(\mu\text{-}OH)](ClO_4)_2 \cdot 2H_2O$ and $[Cu_2(L)(H_2O)_2]PF_6 \cdot H_2O$, were grown by slow evaporation of their methanolic solution. The X-ray intensity data were measured at 293 K on Bruker AXS SMART APEX CCD diffractometer (Mo Kα, $\lambda = 0.71073$ Å). The detector was placed at a distance 6.03 cm from the crystal. A total of 606 frames were collected with a scan width of 0.3° in different settings of φ. The data were reduced in SAINTPLUS,[20] and the empirical absorption correction was applied using the SADABS package.[20] Metal atoms were located by direct methods, and the rest of the non-hydrogen atoms emerged from successive Fourier synthesis. The structures were refined by full matrix least-squares procedure on F^2. All non-hydrogen atoms were refined anisotropically. In complex **2**, the C9 and C25 atoms are found to second-order disorder and solved using part instruction. The H4B atom for **1** and the H4B, H4C, H5A, and H5B atoms in **2** could be located from difference maps and solved using the riding model. The remaining hydrogen atoms were included in the calculated positions. Calculations were performed using the SHELXTL v.6.14[21] program package. Molecular structure plots were drawn using the Oak Ridge thermal ellipsoid plot (ORTEP).[22] Relevant crystal data are given in Table 1.

Catecholase Activity. The catecholase activity has been studied in methanol at 25 °C by reaction of the complexes with 3,5-di-*tert*-butylcatechol (3,5-DTBC). For this purpose a 1.67×10^{-4} M solution of the complexes was treated with 50 equiv of 3,5-DTBC under aerobic condition. The increase in absorption band at 395 nm, characteristic of the quinone formed, was followed spectrophotometrically at various time intervals from 3 to 120 min. The kinetic parameters were evaluated for a 1.67×10^{-4} M solution of the complexes and a 1.67×10^{-4}−8.35×10^{-3} M solution of the substrate in oxygen saturated methanol/aqueous buffer (TRIS, pH 8.5).

Synthesis of Complexes. $[Cu_2(H_2L)(\mu\text{-}OH)](ClO_4)_2$, 1. To a solution of copper(II) perchlorate hexahydrate (0.372 g, 1.0 mmol) in methanol (20 mL) was added H_3L (0.258 g, 0.5 mmol), the resulting brownish green solution was stirred for 0.5 h at room temperature, and then to it was added imidazole (0.068 g, 1.0 mmol) and stirred for another 0.5 h resulting in a dark green solution. Slow evaporation of the solution yielded a green crystalline product. Yield: 0.321 g (72%). Anal. Calcd for $C_{31}H_{44}N_4Cl_2O_{12}Cu_2$: C, 43.16; H, 5.14; N, 6.49. Found: C, 42.98; H, 5.21; N, 6.39. UV−vis (λ_{max}, nm (ε, M^{-1} cm^{-1}); CH_3CN): 280 (6825), 372 (627), 703 (78). IR (KBr, cm^{-1}): $\nu(ClO_4^-)$ 1092, 626; $\nu(O-H_{phenolic})$ 726; $\nu(C-O_{phenoxo})$ 1273. E_{pc} ($Cu^{II}Cu^{II}-Cu^{II}Cu^{I}$ couple): −0.80 V (irr), ($Cu^{II}Cu^{I}-Cu^{I}Cu^{I}$ couple): −1.10 V (irr).

$[Cu_2(L)(H_2O)_2]PF_6$, 2. To a methanolic solution (20 mL) of copper(II) acetate monohydrate (0.200 g, 1.0 mmol) was added H_3L (0.258 g, 0.5 mmol), the resulting solution was stirred for 0.5 h at room temperature, and to it was added NH_4PF_6 and stirred for another 0.5 h resulting in a greenish solution. Slow evaporation of the solution yielded a green crystalline product. Yield: 0.294 g (70%). Anal. Calcd for $C_{31}H_{45}N_4O_5PF_6Cu_2$: C, 45.09; H, 5.49; N, 6.78. Found: C, 45.12; H, 5.34; N, 6.65. UV−vis (λ_{max}, nm (ε, M^{-1} cm^{-1}) CH_3CN): 282 (7230); 411 (680); 717 (139). IR (KBr, cm^{-1}): $\nu(PF_6^-)$ 845; $\nu(C-O_{phenoxo})$ 1273. E_{pc} ($Cu^{II}Cu^{II}-Cu^{II}/Cu^{I}$ couple): −0.83 V (irr), ($Cu^{II}Cu^{I}-Cu^{I}Cu^{I}$ couple): −1.15 V (irr) .

Table 1. Crystal Data and Structure Refinement Parameters for Complex **1** and **2**

	1	**2**
formula	$C_{31}H_{48}Cl_2N_4O_{14}Cu_2$	$C_{31}H_{47}N_4O_6PF_6Cu_2$
fw	898.71	843.78
cryst system	monoclinic	triclinic
space group	$P2_1/c$	$P\bar{1}$
a (Å)	14.898(4)	12.647(3)
b (Å)	12.292(2)	12.816(3)
c (Å)	21.977(5)	13.654(3)
α (deg)	90.000	65.230(3)
β (deg)	105.616(4)	77.540(3)
γ (deg)	90.000	64.37(3)
V (Å^3)	3876.1(16)	1805.4(6)
Z	4	2
D_{calcd} (mg m^{-3})	1.540	1.552
μ (mm^{-1})	1.304	1.300
θ (deg)	1.42 to 25.00	1.65 to 25.00
T (K)	293(2)	293(2)
R1,[a] wR2[b] [$I > 2\sigma(I)$]	0.0715, 0.1992	0.0573, 0.1517
GOF on F^2	1.026	1.042

[a] $R1 = (\Sigma||F_o| - |F_c||)/\Sigma|F_o|$. [b] $wR2 = [\Sigma w(F_o^2 - F_c^2)^2/\Sigma w(F_o^2)^2]^{1/2}$.

Results and Discussion

Synthesis. The N_4O_3 coordinating heptadentate ligand, abbreviated as H_3L, has been used in the present work. The stoichiometric reaction of $Cu(ClO_4)_2 \cdot 6H_2O$ with H_3L in the presence of imidazole afforded the μ-phenoxo, μ-hydroxo bridged binuclear complex of formula $[Cu_2(H_2L)(\mu\text{-}OH)](ClO_4)_2$. However, when $Cu(OAc)_2 \cdot H_2O$ reacted with H_3L in the absence of imidazole, it yielded $[Cu_2(L)(H_2O)_2]PF_6$ upon addition of NH_4PF_6.

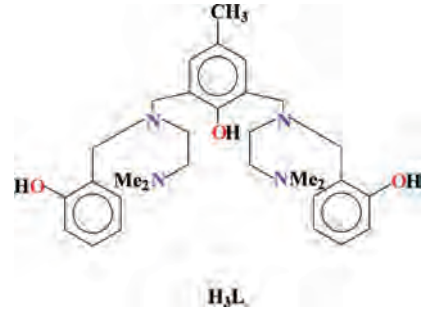

H_3L

IR Spectra. In complex **1**, the Cu(II)−μ-OH−Cu(II) stretch mode is observed at 762 cm^{-1}. The $O-H_{phenol}$ vibration in **1** occurs at 1384 cm^{-1} and is consistent with the bridging of the phenolic oxygen atom without deprotona-

(15) Frisch, M. J.; Trucks, G. W.; Schlegel, H. B.; Scuseria, G. E.; Robb, M. A.; Cheeseman, J. R.; Montgomery, J. A., Jr.;Vreven, T.; Kudin, K. N.; Burant, J. C.; Millam, J. M.; Iyengar, S. S.; Tomasi, J.; Barone, V.; Mennucci, B.; Cossi, M.; Scalmani, G.; Rega, N.; Petersson, G. A.; Nakatsuji, H.; Hada, M.; Ehara, M.; Toyota, K.; Fukuda, R.; Hasegawa, J.; Ishida, M.; Nakajima, T.; Honda, Y.; Kitao, O.; Nakai, H.; Klene, M.; Li, X.; Knox, J. E.; Hratchian, H. P.; Cross, J. B; ammi, R.; Pomelli, C.; Ochterski, J. W.; Ayala, P. Y.; Morokuma, K.; Voth, G. A.; Salvador, P.; Dannenberg, J. J.; Zakrzewski, V. G.; Dapprich, S.; Daniels, A. D.; Strain, M. C.; Farkas, O.; Malick, D. K.; Rabuck, A. D.; Raghavachari, K.; Foresman, J. B.; Ortiz, J. V.; Cui, Q.; Baboul, A. G.; Clifford, S.; Cioslowski, J.; Stefanov, B. B.; Liu, G.; Liashenko, A.; Piskorz, P.; Komaromi, I.; Martin, R. L.; Fox, D. J.; Keith, T.; Al-Laham, A.; Peng, C. Y.; Nanayakkara, A.; Challacombe, M.; Gill, P. M. W.; Johnson, B.; Chen, W.; Wong, M. W.; Gonzalez, C.; Pople, J. A. *Gaussian 03W*, revision C.02; Gaussian, Inc.: Wallingford, CT, 2004.
(16) Becke, A. D. *J. Chem. Phys.* **1993**, *98*, 5648.
(17) Lee, C.; Yang, W.; Parr, R. G. *Phys. Rev. B.* **1998**, *37*, 785.
(18) Schaefer, A.; Huber, C.; Ahlrichs, R. *J. Chem. Phys.* **1994**, *100*, 5829.
(19) Schaefer, A.; Horn, H.; Ahlrichs, R. *J. Chem. Phys.* **1992**, *97*, 2571.
(20) *SMART, SAINT, SADABS, XPREP, SHELXTL*; Bruker AXS Inc.: Madison, WI, 1998.
(21) Sheldrick, G. M. *SHELXTL*, v.6.14; Bruker AXS Inc.: Madison, WI, 2003.
(22) Johnson C. K. *ORTEP*; Report ORNL-5138; Oak Ridge National Laboratory: Oak Ridge, TN, 1976.

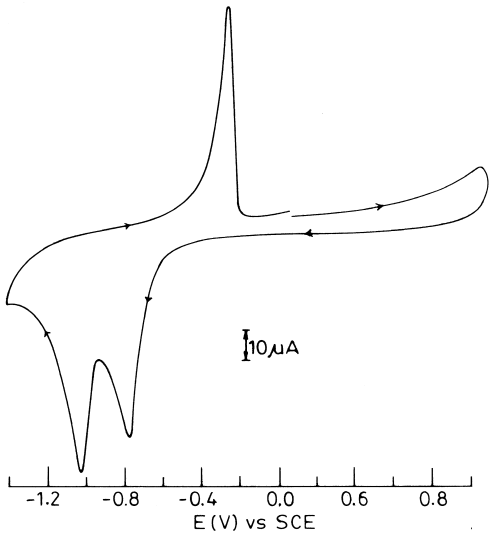

Figure 1. Cyclic voltammograms of a $\sim 10^{-3}$ M solution of $[Cu_2(H_2L)(\mu\text{-}OH)](ClO_4)_2$ in acetonitrile solution.

tion.[23] No such stretches were observed in case of **2** which suggests that the terminal phenolic oxygen atom coordinated as phenoxide. In both cases, $\nu(C-O_{(phenoxo)})$ appears at 1273 cm^{-1}.[24] The ClO_4^- vibrations for **1** and PF_6^- vibrations for **2** occur at 1092, 626 and 845 cm^{-1}, respectively.

UV−vis Spectra. The UV−vis spectra of the complexes were recorded in an acetonitrile (CH_3CN) solution and display two well resolved peaks along with a shoulder. The absorption near 400 nm is probably due to a Cu(II) → phenolate(axial) metal-to-ligand charge transfer (MLCT) or a phenolate(equatorial) → Cu(II) ligand-to-metal charge transfer (LMCT) transition.[25] In both cases a d−d band appears near 710 nm, and the position of the d−d band and the low energy shoulder suggest that the geometry around the copper(II) ion is best described as square pyramidal.[26] Similar absorption was observed for other (μ-phenoxo) dicopper(II) complexes.[5a,b,g,7d]

Electrochemical Study. All the complexes are electroactive in acetonitrile solution versus SCE. The complexes exhibit two cathodic waves at −0.80 and −1.10 V. The first couple is assigned to the $Cu^{II}Cu^{II}$ to $Cu^{II}Cu^{I}$ reduction, whereas that of the second is assigned to the $Cu^{II}Cu^{I}$ to $Cu^{I}Cu^{I}$ reduction. In addition, there is a characteristic feature of a redissolution process, and it is believed that the two electron reduction causes a partial decomplexation and release of Cu^+ ions which in turn undergo further reduction from Cu^{I} to Cu^0 leading to a deposition of Cu metal at the electrode surface. The electrodeposited copper is redissolved and characterized by a sharp anodic stripping at −0.30 V (Figure 1). Such electrochemical behavior is consistent with

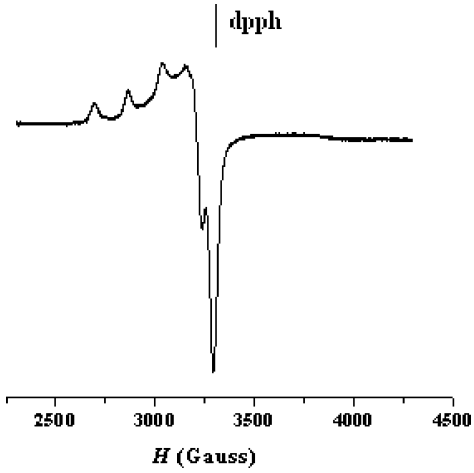

Figure 2. X-band EPR spectra for $[Cu_2(L)(H_2O)_2]PF_6$ in solid state at 77 K. Instrument settings: microwave frequency, 9.1 GHz; microwave power, 30 dB; modulation frequency, 100 kHz; modulation amplitude, 12.5 G; sweep centre, 3200 G.

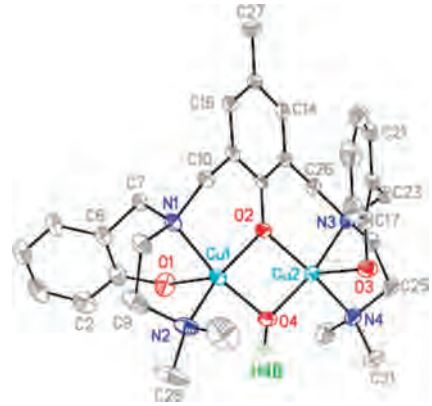

Figure 3. ORTEP plot and atom-labeling scheme of the cationic part of $[Cu_2(H_2L)(\mu\text{-}OH)](ClO_4)_2$. All non-hydrogen atoms are represented by their 30% thermal probability ellipsoids.

the other reported binuclear copper complexes using binuclear complex forming ligands.[3f,6b,7d]

EPR Spectra. Complex **1** is EPR silent both in solution and in solid state. In frozen solution, the EPR spectra of complex **2** is given in Figure 2. The spectrum is characterized by an axial pattern with the features $g_{\|} > 2.1 > g_{\perp} > 2$ ($g_{\|} = 2.218$, $g_{\perp} = 2.04$) and the $A_{\|} = 168 \times 10^{-4}$. This result is consistent with the tetragonally elongated square pyramid geometry around the copper ion for uncoupled or weakly coupled Cu(II) ions.[27]

Crystal Structure. The crystal structure of $[Cu_2(H_2L)(\mu\text{-}OH)](ClO_4)_2 \cdot 2H_2O$ (**1**) and $[Cu_2L(OH_2)_2]PF_6 \cdot H_2O$ (**2**) have been determined. A view of the cationic part of the binuclear entity in both cases is shown in Figures 3 and 4, respectively. The important interatomic distance parameters and angles are listed in Table 2.

In complex **1**, the two Cu-centers are bridged by the hydroxo oxygen atom (Cu1−O4−Cu2 = 102.6°) and the central phenolato oxygen atom (Cu1−O2−Cu2 = 100.63°) leading to a mixed bridged binuclear species with Cu1···Cu2,

(23) Neves, A.; Rossi, L. M.; Horn, A., Jr; Vencato, I.; Bortoluzzi, A. J.; Zucco, C.; Mangrich, S. *Inorg. Chem. Commun.* **1999**, *2*, 334.
(24) Nakamoto, K. *Infrared and Raman Spectra of Inorganic and Coordination Compounds*, 4th ed.; John Wiley & Sons: New York, 1986; p 191.
(25) Vidyanathan, M.; Viswanathan, R.; Palaniandavar, M. *Inorg. Chem.* **1998**, *37*, 6418.
(26) (a) Karlin, K. D.; Hayes, J. C.; Juen, S.; Hutchinson, J. P.; Zubieta, J. *Inorg. Chem.* **1982**, *21*, 4106. (b) Addison, A. W.; Hendriks, H. M. J.; Reedijk, J.; Thompson, L. K. *Inorg. Chem.* **1981**, *20*, 103. (c) Hathaway, B. J.; Billing, D. E. *Coord. Chem. Rev.* **1970**, *5*, 143.
(27) Hathaway, B. J. In *Comprehensive Coordination Chemistry*; Wilkinson, G., Gillard, R. D., McCleverty, J. A., Eds.; Pergamon Press: Oxford, U.K., 1987; Vol. 5, p 668.

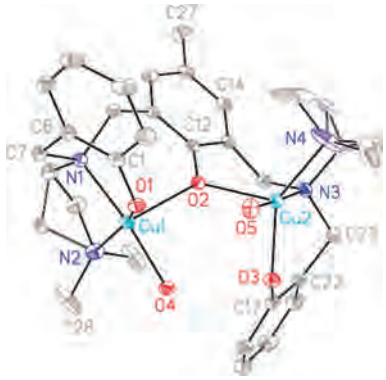

Figure 4. ORTEP plot and atom-labeling scheme of the cationic part of $[Cu_2(L)(H_2O)_2]PF_6$. All non-hydrogen atoms are represented by their 30% thermal probability ellipsoids.

2.9893(12) Å. In the Cu_2O_2 core, the two copper atoms and the two oxygen atoms are on a plane (md 0.0188 Å), and the Cu−O bond distances fall in the range of 1.91−1.94 Å. In the coordination environment, each copper atom has a distorted square pyramidal geometry ($\tau = 0.01 - 0.205$),[28] and the equatorial position is occupied by two nitrogen and two bridging oxygen atoms. The remaining phenolic OH group of the ligand completed the coordination sphere of the apical sites on each copper ion in an anti configuration. In the CuO_3N_2 coordination sphere, the metal atoms are displaced toward the phenolic oxygen atom by 0.2368 Å for the Cu1 atom and 0.1269 Å for the Cu2 atom. The Cu−N bond distances span in the range 1.97−2.10 Å, which confirms its equatorial binding.

In complex **2**, the ligand binds in a trianionic form where the two copper atoms are bridged by a central phenoxo group, Cu1−O2−Cu2 = 121.74°, and the Cu ··· Cu distance is 3.747 Å. In this case, the geometry of the two copper ions is different, and the geometry around the Cu1 atom is distorted square pyramidal whereas that of Cu2 is likely to be square based pyramidal distorted trigonal bipyramidal[28] ($\tau = 0.54$). The other Cu−O and Cu−N bond distances are as usual.

Magnetic Properties and Electronic Structure. The magnetic susceptibility for both the complexes has been obtained in the temperature range 2−300 K. The $\chi_M T$ versus T plot for complexes **1** and **2** are given in Figures 5 and 6, respectively. The experimental data were fitted using the Hamiltonian $\hat{H} = -J\hat{S}_1\hat{S}_2$.

The magnetic properties of complex **1** show a strong antiferromagnetic interaction between the two copper ions with $J = -372$ cm^{-1}. In complex **1**, two copper ions are linked equatorially via a bridging hydroxo and a phenoxo group. For the hydroxo bridged binuclear copper(II) complexes, they exhibit ferromagnetic or antiferromagnetic interactions mainly regulated by the Cu−O−Cu bond angle (θ) and the out-of-plane displacement of the hydrogen of the bridging hydroxo group from the Cu_2O_2 plane. The complexes show antiferromagnetic behavior at θ greater than 90°[29a,b] and the out-of-plane displacement of the hydroxo bridged hydrogen less than 50°.[29c–e] In complex **1**, Cu1−μ(OH)−Cu2 and Cu1−O(phenoxo)−Cu2 angles are 102.6° and 100.63°, respectively, and the out-of-plane displacement of the hydroxo bridge hydrogen atom is 17.8° (O2−O4−H4B = 163.3°). Thus, the experimentally observed exchange coupling constant is in good agreement with the structural features of the molecule.

Complex **2** exhibits very weak intramolecular antiferromagnetic interactions with $J = -2.76$ cm^{-1}. It has been cited in the literature that binuclear Cu(II) complexes linked by bridging groups coordinated axially exhibit very weak antiferromagnetic or ferromagnetic or no exchange interaction.[5f] In complex **2**, the bridging phenoxide group is coordinated axially to both the copper centers, which explains the very low exchange coupling constant.

The spin density calculated for the triplet state from a DFT study provides valuable insights for understanding the behavior of the unpaired electron and hence the exchange coupling between the two metal centers.[8d,29,30] Larger delocalization generally means better overlap between the magnetic orbitals of the metal ions through the suitable orbital of the bridging ligand which favors the antiferromagnetic interaction.[8d,30d] The degree of delocalization of the unpaired electron increases if the coordinating atoms of the ligand participate in the singly occupied molecular orbital (SOMO), which leads to the enhancement of the electron density of the donor atoms. Interestingly, in both cases the spin density is mainly distributed among the copper $d_{x^2-y^2}$ magnetic orbital and the donor atoms coordinated equatorially. It is to be noted that the calculated exchange coupling constant for **2** using the crystal coordinates gives weak ferromagnetic interaction ($J = 2.56$ cm^{-1}). Thus, in the case of **2** all the DFT calculation were performed using the optimized geometry. For the optimized geometry, the calculated (UB3LYP) average Cu-μ-O(phenoxo) bond length is 2.13 Å, which is comparable with the average X-ray value (2.14 Å). The other bond distances within the coordination sphere are marginally deviated from the experimentally observed values. In terms of magnetic properties, the Cu1−μ-O(phenoxo)−Cu2 angle is the most important, and this angle is smaller by ≈3 deg (118.49) in the optimized geometry (Supporting Information, Table S1) The calculated spin density in the triplet state for the two complexes is given in Table 3. The calculated exchange coupling constants using different basis sets are listed in Table 4.

In addition, the energies of the singly occupied molecular orbitals in the triplet state are also very useful to compare

(28) O'Sullivan, C.; Murphy, G.; Murphy, B.; Hathaway, B. *J. Chem. Soc., Dalton Trans.* **1999**, 1835.

(29) (a) Hodgson, D. J. *Prog. Inorg. Chem.* **1975**, *19*, 173. (b) Crawford, V. H.; Richardson, H. W.; Wasson, J. R.; Hodgson, D. J.; Hatfield, W. E. *Inorg. Chem.* **1976**, *15*, 2107. (c) Ruiz, E.; Alemany, P.; Alvarez, S.; Cano, J. *J. Am. Chem. Soc.* **1997**, *119*, 1297. (d) Rodriguez-Fortea, A.; Ruiz, E.; Alvarez, S.; Alemany, P. *Dalton Trans.* **2005**, 2624. (e) Hu, H.; Liu, Y.; Zhang, D.; Liu, C. J. *Mol. Struc.(Theor. Chem.).* **2001**, *546*, 73.

(30) (a) Cano, J.; Ruiz, E.; Alvarez, S.; Verdaguer, M. *Comments Inorg. Chem.* **1998**, *20*, 27. (b) Cano, J.; Alemany, P.; Alvarez, S.; Verdaguer, M.; Ruiz, E. *Chem.—Eur. J.* **1998**, *4*, 476. (c) Cano, J.; Rodríguez-Fortea, A.; Alemany, P.; Alvarez, S.; Ruiz, E. *Chem.—Eur. J.* **2000**, *6*, 327. (d) Barone, V.; Bencini, A.; Gatteschi, D.; Totti, F. *Chem.—Eur. J.* **2002**, *8*, 5019. (e) Desplanches, C.; Ruiz, E.; Rodríguez-Fortea, A.; Alvarez, S. *J. Am. Chem. Soc.* **2002**, *124*, 5197.

Table 2. Selected Bond Distances (Å) and Angles (deg) for Complexes **1** and **2**

	1	2		1	2
			Distances		
Cu1−O1	2.296(5)	1.976(3)	Cu2−O3	2.361(5)	1.999(3)
Cu1−O2	1.943(4)	2.182(3)	Cu2−O4	1.913(5)	
Cu1−O4	1.916(5)	1.946(3)	Cu2−O5		2.003(3)
Cu1−N1	2.009(5)	1.979(4)	Cu2−N3	2.000(5)	2.023(4)
Cu1−N2	2.001(6)	2.064(4)	Cu2−N4	2.012(6)	2.041(5)
Cu2−O2	1.942(4)	2.107(3)	Cu1···Cu2	2.9893(12)	3.747(8)
			Angles		
O1−Cu1−O2	101.5(2)	98.36(13)	O2−Cu2−N3	91.81(18)	94.71(14)
O1−Cu1−O4	97.5(2)	85.65(14)	O2−Cu2−N4	169.3(2)	119.4(3)
O1−Cu1−N1	88.6(2)	94.40(14)	O3−Cu2−O4	96.2(2)	
O1−Cu1−N2	100.2(3)	158.25(17)	O3−Cu2−O5		87.68(14)
O2−Cu1−O4	78.28(19)	92.08(13)	O3−Cu2−N3	87.77(19)	96.42(14)
O2−Cu1−N1	92.96(18)	94.50(14)	O3−Cu2−N4	95.7(2)	141.5(3)
O2−Cu1−N2	158.4(2)	103.37(16)	O4−Cu2−N3	169.7(2)	
O4−Cu1−N1	170.1(2)	173.33(15)	O4−Cu2−N4	100.7(2)	
O4−Cu1−N2	98.8(2)	92.43(16)	O5−Cu2−N3		173.72(15)
N1−Cu1−N2	87.7(2)	85.04(16)	O5−Cu2−N4		89.09(19)
O2−Cu2−O3	95.00(18)	98.90(13)	N3−Cu2−N4	88.4(2)	84.7(2)
O2−Cu2−O4	78.38(18)		Cu1−O2−Cu2	100.63(18)	121.74(14)
O2−Cu2−O5		89.33(13)	Cu1−O4−Cu2	102.6(2)	

the exchange coupling constant qualitatively as proposed by Hay et al.[31] According to the model, the antiferromagnetic exchange coupling constant for the binuclear metal complexes, each bearing one unpaired electron, is linearly proportional to the square of the energy difference between the two SOMOs.

In complex **1**, there is considerable amount of distribution of spin into the bridging oxygen atoms (Table 3). It is also clear from the spin density plot, Figure 7, that the overlap between the magnetic orbitals of the copper atoms is taking place via the bonding between the $d_{x^2-y^2}$magnetic orbital of copper and the hybrid orbital of the bridging oxygen atoms. Thus, the spin delocalization on the bridging group corroborates the strong antiferromagnetic interaction. Moreover, the significant overlap between the magnetic orbitals through the bridging groups enhances the energy separation (0.02667 eV) between the SOMOs. The large energy separation between the SOMOs in the triplet state also support the strong antiferromagnetic exchange coupling constant.[31]

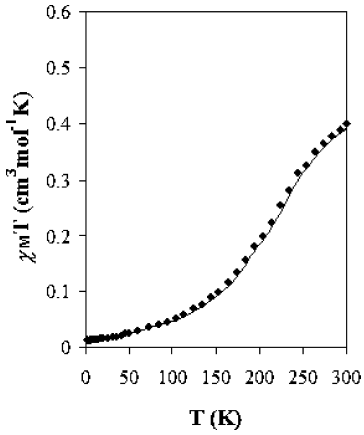

Figure 5. $\chi_M T$ versus T for **1**. Open points are the experimental data and the solid line represents the best fit obtained.

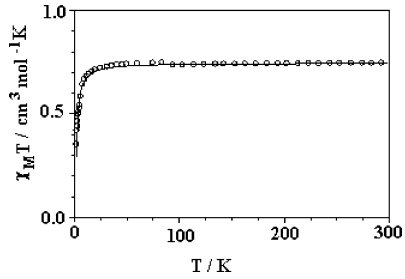

Figure 6. $\chi_M T$ versus T for **2**. Open points are the experimental data and the solid line represents the best fit obtained.

The DFT calculation using the optimized geometry predicts the weak antiferromagnetic interaction $J = -6.52$ cm^{-1} in the case of **2**. The weak antiferromagnetism may be explained by considering the distribution of the spin density of the triplet state (Table 3). The calculated spin density of the bridging oxygen atom is 0.0088, which is also reflected in the spin density plot (Figure 8) and corresponds to the triplet state. The low spin density on the bridging atom results in negligible overlap between the magnetic orbital of the metal ion and the hybrid orbital of the bridging oxygen atom. However, it is believed that the through space overlap[30e] between the magnetic orbitals is probably responsible for the weak antiferromagnetic exchange coupling. In this case the marginal energy difference (0.00853 eV) between the two SOMOs in the triplet state is also a signature of a very weak antiferromagnetic interaction.

In summary, the delocalization of the unpaired electrons through the bridging atoms and the larger energy separation between the two SOMOs in **1** compared to that of **2** is attributed to the strong antiferromagnetic coupling for complex **1**. Thus, the theoretical results matched well with the experimental findings.

Catecholase Activity. Both the complexes show efficient catecholase activity in the oxygen saturated methanolic solution. At first a pH dependent study was done in the range 6−10 to determine the optimum pH at which the complexes show their maximum catecholase activity. To minimize the effect of pH on the spontaneous reaction the same solution was used without adding the complexes as an internal reference. In both cases there is a slow increase of catalytic

Table 3. Calculated Mulliken Spin Densities for the Complexes **1** and **2**[a]

complex	Cu	μ-$O_{phenoxo}$	μ-$O_{hydroxo}$	N	$O_{phenoxo}$	$O_{phenolato}$	O_{aqo}
1	0.5855	0.1424	0.1347	0.1271		0.0021	
2	0.5854	0.0088		0.1176	0.0884		0.0537

[a] Triple-ζ quality all-electron basis set for copper atoms (TZP) and a double-ζ all-electron basis set for other atoms with B3LYP hybrid function.

Table 4. Calculated Exchange Coupling Constants J (cm^{-1}) for **1** and **2** Using Different Basis Sets

complex	Cu basis set	C, N, and O	H	J_{Calc} (cm^{-1})	J_{Exp} (cm^{-1})
1	ae TZP	aeDZ	6−31G	−455	−372
	Ps LANL2DZ	aeDZ	6−31G	−500	−372
	ae TZP	aeDZ	6−31G	−6.52	−2.76
2	Ps LANL2DZ	aeDZ	6−31G	−7.24	−2.76

activity up to pH 7.5. Further increase of pH results in sharp rise of their reactivity up to pH 8.5. Beyond pH 9.0, no appreciable change is observed (Figure 9). Therefore, the oxidation reaction was carried out at pH 8.5. It has been found that the catechol oxidases show maximum activity at pH 8.[32] In alkaline medium, the metal coordinated hydroxide group probably is able to interact with the 3,5-DTBC facilitating the deprotonation of the substrate and the subsequent binding to the metal centers before its oxidation.

Before starting the detailed kinetic study, the ability of the complexes toward oxidation of catechol to quinone was examined, and the time dependent growth of 3,5-DTBQ in case of **2** is shown in Figure 10. The increase in the concentration of quinone with when time catalyzed by complex **2** is plotted in Figure 11.

The kinetic study of the oxidation of 3,5-DTBC to 3,5-DTBQ by the complexes was carried out by monitoring the increase of absorption of quinone at 395 nm by the initial rate (V_0) method.

There is a linear relationship between the initial rate and the concentration of the substrate indicating the first order dependence on the 3,5-DTBC concentration for this system. Saturation kinetics were found for the initial rates versus the 3,5-DTBC concentration for the complexes and are shown in Figure 12. An analysis of the data on the basis of the Michaelis−Menten approach,[3c,e,33] originally developed for enzyme kinetics, was applied.

Figure 7. Spin density plot corresponds to the triplet state for **1** (isosurface cutoff value = 0.002).

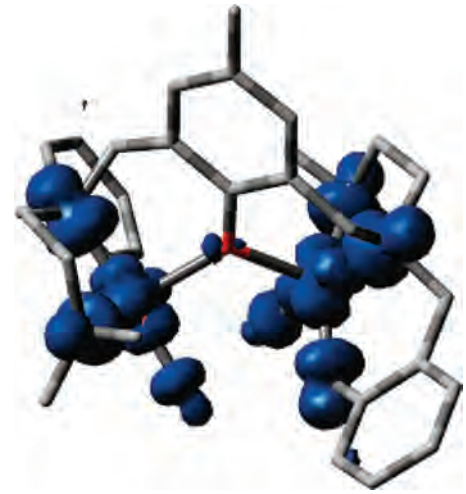

Figure 8. Spin density plot for the triplet state of 2 (isosurface cutoff value = 0.002).

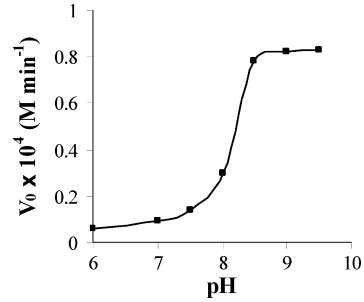

Figure 9. Dependence of the initial reaction rates on pH for the oxidation of 3,5-DTBC catalyzed by complex **1**. The reactions were performed in methanol saturated with O_2/aqueous buffer (TRIS/HCl pH 6.0, 7.0 and TRIS pH 7.5, 8.0, 8.5, 9.0 and NaOH pH 9.5) [Complex] = 1.6×10^{-4} M and [3,5-DTBC] = 8.0×10^{-3} M at 25 °C.

The Lineweaver−Burk plot for complex **1** is given in Figure 13, and the parameters obtained for both complexes are given in Table 5. Complexes **1** and **2** show a turnover rate of about 29 and 37 h^{-1}, respectively. The values of the kinetic parameters are in the range of those observed for other binuclear copper complexes[3c,f,6b,7c,d,34] synthesized using other binucleating ligand systems, and thus, the compounds **1** and **2** can be considered as functional model for catechol oxidase.

(31) Hay, P. J.; Thibeault, J. C.; Hoffmann, R. *J. Am. Chem. Soc.* **1975**, *97*, 4884.
(32) Rompel, A.; Fischer, H.; Meiwes, D.; Buldt-Karentzopoulos, K.; Dillinger, R.; Tuczek, F.; Witzel, H.; Krebs, B. *J. Biol. Inorg. Chem.* **1999**, *4*, 56.
(33) Than, R.; Feldman, A. A.; Krebs, B. *Coord. Chem. Rev.* **1999**, *182*, 211.
(34) (a) Neves, A.; Rossi, L. M.; Bortoluzzi, A. J.; Szpoganicz, B.; Wiezbicki, C.; Schwingel, E.; Hasse, W.; Ostrovsky, S. *Inorg. Chem.* **2002**, *41*, 1788. (b) Koval, I. A.; Patrick, G.; Belle, C.; Selmeczi, K.; Reedijk, J. *Chem. Soc. Rev.* **2006**, *35*, 814.

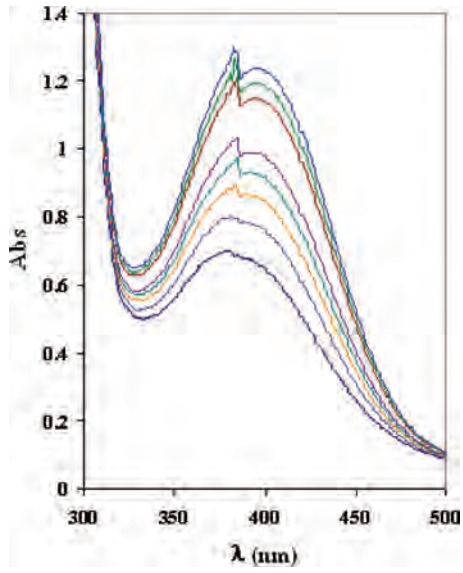

Figure 10. Time dependent growth of 3,5-DTBQ at 395 nm in methanol, 25 °C.

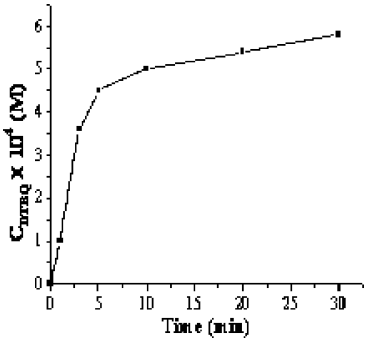

Figure 11. Plot of concentration of 3,5-DTBQ vs time.

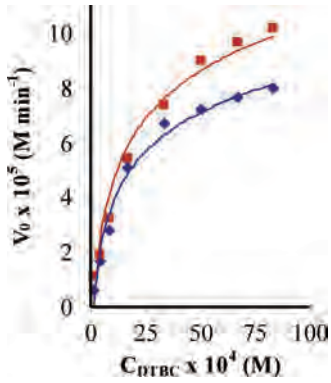

Figure 12. Dependence of the initial reaction rates on the 3,5-DTBC concentration for the oxidation reaction catalyzed by dicopper (II) complexes (◆) 1; (■) 2.

The geometry around the copper ions and the distance between them are assumed to be the key factors that determine the catalytic activity of the complexes.[6b,35] In present system, the Cu···Cu distance in complex **2** is 3.747 Å which is much greater than that of **1** (Cu···Cu, 2.9893 Å). The inter metallic distance in **1** is closer to the distance of 3.25 Å reported for *o*-catecholato bridged dicopper complex.[36] So apparently it is expected that the rate of catechol oxidation by **1** will be higher than by **2**. However, we observed that the turnover rate for complex **2** is higher than that of complex **1**. It has been cited in the literature[34b] that for the pH dependence oxidation reactions the coordination of diphenol as a bridging ligand prior to intermolecular electron transfer leads to the formation of quinone. For complex **1**, the axial phenolic OH groups are *trans* to each other, and this geometry hinders the approach of 3,5-di-*tert*-butylcatechol toward the copper centers, thus retarding the rate of oxidation.

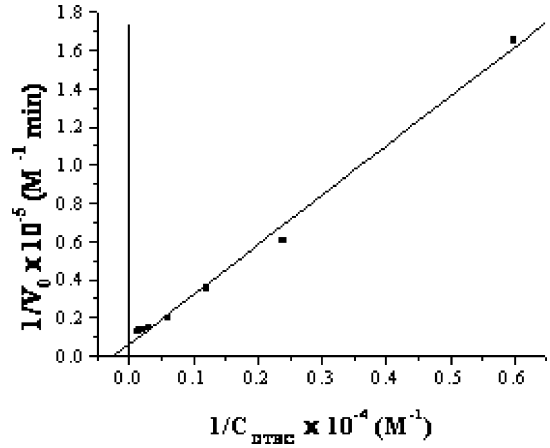

Figure 13. Lineweaver−Burk plot for aerobic oxidation of 3,5-DTBC by complex **1**.

Table 5. Kinetic Parameters

complex	V_{max} (M min^{-1})	K_M (M)	k_{cat} (min^{-1})
1	8.0×10^{-5}	11.6×10^{-4}	0.479
2	10.15×10^{-5}	12.2×10^{-4}	0.608

It has been observed that the rate of the reaction decreases with time in both cases. It has also been known that the free copper ion catalyzes the oxidation of catechol to quinone in the presence of oxygen in the pH range 6.6−6.8,[37] and the rate decreases substantially with increasing pH and concentration of catechol. In our case, the complexes show maximum catalytic activity at about pH 8.5 which indicates that the involvement of the free copper ion in the oxidation process is insignificant. However, the observed decrease in the rate of oxidation with time can be attributed either to the transformation of the active form to the less reactive Cu(3,5-DTBC) or $[Cu(3,5\text{-}DTBC)_2]^{2-}$ species in presence of excess catechol or to the formation of 3,5-di-*tert*-butylquinone(3,5-DTBQ).[37,38]

Conclusion

We have prepared and characterized two binuclear Cu(II) complexes of formula $[Cu_2(H_2L)(\mu\text{-}OH)](ClO_4)_2$ (**1**) and

(35) (a) Albedyhl, S.; Averbuch-Pouchot, M. T.; Belle, C.; Krebs, B.; Pierre, J. L.; Saint-Aman, E.; Torrelli, S. *Eur. J. Inorg. Chem.* **2001**, *40*, 1457. (b) Belle, C.; Beguin, C.; Gautier-Luneau, I.; Hamman, S.; Philouze, C.; Pierre, J. L.; Thomas, F.; Saint-Aman, E.; Bonin, M. *Inorg. Chem.* **2002**, *41*, 479. (c) Mukherjee, J.; Mukherjee, R. *Inorg. Chim. Acta* **2002**, *337*, 429.

(36) Karlin, K. D.; Gultneh, Y.; Nicholson, T.; Zubieta, J. *Inorg. Chem.* **1985**, *24*, 3727.

(37) Kamau, P.; Jordan, R. B. *Inorg. Chem.* **2002**, *41*, 3076.

(38) Koval, I. A.; Selmeczi, K.; Belle, C.; Philouze, C.; Saint-Aman, E.; Gautier-Luneau, I.; Schuitema, A. M.; van Vliet, M.; Gamez, P.; Roubeau, O.; Lüken, M.; Krebs, B.; Lutz, M.; Spek, A. L.; Pierre, J. L.; Reedijk, J. *Chem.—Eur. J.* **2006**, *12*, 6138.

$[Cu_2(L)(H_2O)_2]PF_6$, (**2**) incorporating a N_4O_3 coordinating heptadentate ligand. In complex **1**, two copper(II) centers are linked by μ-phenoxo and μ-hydroxo bridged whereas those of **2** are held by a μ-phenoxo bridge. The variable temperature magnetic moment confirms the strong and weak antiferromagnetic interaction in **1** and **2**, respectively. The exchange interaction for both cases has been determined using DFT-BS. Both complexes exhibit catecholase activity, and the steric factor contributes toward the retardation of the rate of oxidation of catechol to quinone by **1** compared to that by **2**. In summary, the study presented herein provides valuable insights into the biologically relevant coordination chemistry of copper. Further research aimed at the synthesis of polynuclear copper complexes and a theoretical investigation of their physical properties, as well as the interaction with different biomolecules using different polydentate ligands, is currently in progress.

Acknowledgment. Financial support from the Department of Science and Technology, New Delhi, India and the Council of Scientific and Industrial Research, New Delhi, India, University Grant Commission, New Delhi is greatly acknowledged. We are thankful to DST for the data collection on the CCD facility setup (Indian Institute of Science, Bangalore, India) under the IRHPA-DST program.

Supporting Information Available: X-ray crystallographic file in CIF format for $[Cu_2(H_2L)(\mu\text{-}OH)](ClO_4)_2 \cdot 2H_2O$ and $[Cu_2L(OH_2)_2]PF_6 \cdot H_2O$ and a table with calculated bond distances and angles for complex **2** (PDF). This material is available free of charge via the Internet at http://pubs.acs.org.

IC7015935